

## The Effect of the Fin Length on the Solidification Process in a Rectangular Enclosure with Internal Fins

Laila Khatra<sup>1,\*</sup>, Hamid El Qarnia<sup>1</sup> and Mohammed El Ganaoui<sup>2</sup>

**Abstract:** The aim of the proposed work is to study the solidification process within a rectangular enclosure provided with three internal rectangular fins attached to the left vertical wall of the cavity. This latest is filled with a phase change material (PCM), initially liquid, at a temperature above its melting temperature. The solidification process was initiated by cooling the left wall and fins to a temperature lower than the melting temperature. In order to study and examine the thermal behavior and thermal performance of the proposed system, a mathematical model, based on the conservation equations of mass, momentum and energy was developed. The governing equations and their associated boundary and initial conditions were next adimensionalized. Therefore, several controlling parameters were appeared. The volume control method was used to discretize the equations. The resulting algebraic equations were solved iteratively. Numerical investigations were carried out to study and examine the effect of the dimensionless fin length on the hydrodynamic and thermal fields of the flow, the dimensionless heat flux, the solidified mass fraction and the dimensionless time of complete solidification.

**Keywords:** Phase change material, solidification, enthalpy method, fins, rectangular enclosure.

### Nomenclature

$A$	aspect ratio of the enclosure, $H/L$
$x, y$	Cartesian coordinates (m)
$l_0$	characteristic length (m)
$\bar{C}, b$	constants
$X, Y$	dimensionless Cartesian coordinates, $x/l_0, y/l_0$
$\bar{L}_f$	dimensionless fin length, $L_f / l_0$
$\bar{e}_f$	dimensionless fin thickness, $e_f / l_0$

<sup>1</sup> Cadi Ayyad University, Faculty of Sciences Semlalia, Department of Physics, P.O. 2390, Fluid Mechanics and Energetic (affiliated to CNRST, URAC 27), Marrakesh, Morocco.

<sup>2</sup> Lorraine University, Energetic Laboratory of Longwy, (FJV/LERMAB), Henri Poincaré Institute of Longwy, France.

\*Corresponding Author: Laila Khatra. Email: khatra87@gmail.com.

$q$	dimensionless heat flux, $q = \int_{\text{Left wall+Fins}} \frac{\partial \theta}{\partial n} d\eta$
$P$	dimensionless pressure, $p/\rho(\alpha_{m,l}/l_0)^2$
$R_{th}$	dimensionless thermal resistance, $R_{th} = (\theta_m - \theta_c)/q$
$U, V$	dimensionless velocity components, $u/(\alpha_{m,l}/l_0), v/(\alpha_{m,l}/l_0)$
$L_f$	fin length (m)
$H$	height of the enclosure (m)
$L$	length of the enclosure (m)
$f$	liquid mass fraction
$T_m$	melting temperature (K)
$Pr$	Prandlt number, $\nu_{m,l} / \alpha_{m,l}$
$p$	pressure (Pa)
$Ra$	Rayleigh number, $g\beta l_0^3 (T_i - T_m) / (\nu_{m,l} \alpha_{m,l})$
$S$	source term
$c$	specific heat at constant pressure ( $J.kg^{-1}.K^{-1}$ )
$Ste$	Stefan number, $c_{m,l} (T_i - T_m) / \Delta H$
$k$	thermal conductivity ( $W.m^{-1}.K^{-1}$ )
$t$	time (s)
$u, v$	velocity components ( $m.s^{-1}$ )

**Greek Symbols**

$\nu$	cinematic viscosity ( $m^2.s^{-1}$ )
$\rho$	density ( $kg.m^{-3}$ )
$\Psi$	dimensionless stream function
$\overline{\delta_f}$	dimensionless fin- bottom wall distance, $\delta_f/l_0$
$\overline{\lambda_f}$	dimensionless fin spacing, $\lambda_f / l_0$
$\tau_d$	dimensionless solidification time
$\theta$	dimensionless temperature
$\Delta\tau$	dimensionless time step
$\tau$	dimensionless time, $(\alpha_{m,l} t)/l_0^2$
$\beta$	dissipation coefficient ( $K^{-1}$ )
$\mu$	dynamic viscosity ( $kg.m^{-1}.s^{-1}$ )
$\delta_f$	fin- bottom wall distance (m)
$\lambda_f$	fin spacing (m)
$\Delta H$	latent heat of phase change ( $J.kg^{-1}$ )
$\gamma$	ratio of the dimensionless heat fluxes
$\alpha$	thermal diffusivity, $k/\rho c$ ( $m^2.s^{-1}$ )
$\Gamma, \Phi$	variables

**Subscripts**

$m$	average or PCM
-----	----------------

C	cold wall
f	fin
i	initial
l	liquid phase
$\eta$	peripheral distance
ref	reference
s	solid phase
w	wall

## **1 Introduction**

The solid-liquid phase change of pure material is characterized by the transformation, at constant temperature, from a liquid phase to a solid phase or vice versa. This reversible reaction is accompanied by the storage (melting) or the release (solidification) of energy. The solid-liquid phase change processes are encountered in many engineering and industrial applications, such as the solidification of pure metals or alloys, the formation of fine crystals used in electronic systems, the recovery of waste heat from industrial processes, the storage of solar energy during the day using the latent heat storage systems (LHSS), etc. The latent heat storage is more advantageous than the sensible thermal energy storage. Compared to the sensible heat storage systems (SHSS), LHSS are characterized by high energy density and allow nearly constant temperature energy storage. Several studies regarding solid-liquid phase change process were carried out and reported in the literature. The reader can refer to some of these works [Arid, KousKsou, Jegadheeswaran et al. (2012); Semma, El Ganaoui, Timchenko et al. (2006); Rady and Arquis (2010)].

However, most of the phase change materials (PCMs) have low thermal conductivity, which reduces the heat transfer during phase change processes. Several techniques have been investigated in order to enhance the heat transfer in LHSS. Works dealing with the various techniques for increasing heat transfer to promote solidification (or melting) of PCMs are available in the literature cited by Jegadheeswaran et al. [Jegadheeswaran and Pohekar (2009)]. These techniques are summarized as follows: i) Employing multiple PCMs method, ii) Impregnation of porous material; iii) Dispersion of high conductivity particles in the PCM, iv) Use of high conductivity and low density materials, v) Microencapsulation of PCM, vi) Placing of metal structures inside the PCM, vii) Use of the extended surfaces.

The proposed study is focused on the use of fins to enhance heat transfer in a low PCM thermal conductivity during the solidification process. Most investigators have reported that the increase of the surface of heat transfer will improve the heat transfer. Numerical and experimental studies have been made by Velraj et al. [Velraj, Seeniraj, Hafner et al. (1997)] to examine the effect of internal longitudinal fins on the solidification process of the paraffin (RT60) within a vertical cylinder. The results show that introducing fins enhanced more heat transfer and reduced complete time of solidification. The effect of increasing the number of fins was more remarkable for larger tube radius. Ismail et al. [Ismail, Alves and Modesto (2001)] studied the effect of control parameters of the fins in the tubes. The results showed that the fin length and the number of fins as well as the

aspect ratio of the annular space have a great effect on the complete solidification time and the solidification rate. However, the fin thickness has a relatively small influence on the solidification time and the solidification rate. Stritih [Stritih (2004)] reported the enhancement of heat transfer with rectangular external fins in rectangular storage system during the phase change processes (melting and solidification). Compared to the melting process, where the heat transfer is enhanced by natural convection, the solidification process can be strongly enhanced with fins since the sole mode of heat transfer is conduction. To compare the heat transfer with and without fins in a rectangular module, the author estimated the fin effectiveness, which is defined as the ratio of the heat flux with fins to that without fins, experimentally and showed that the fin effectiveness was significantly high and 40% of reduction in solidification time was observed. Approximate analytical solutions were found by Bauer [Bauer (2011)] for solidification of PCMs in finned geometries, finned plane wall and finned tube on the outside, using the average effective properties. The solidification time of the two basic geometries is examined by analytical modeling and numerical computation. The authors mentioned that the analytical models are applicable to a wide range of geometries and typical utilized PCMs. The modeling, which was based on the solidification process, was also applicable to the melting one, if the free convection in the melt is neglected. The work identified different characteristic dimensionless parameters, such as the spacing, the thickness and the number of fins as well as the distance of the finned tubes, and their impact on the solidification time. A computational study has been conducted by Ye et al. [Ye, Zhu and Wang (2011)] to investigate the processes of the latent thermal energy storage/release in a finned plate unit with uniform temperature on heating/cooling plate wall. The impact of temperature differences between the melting temperature of PCM and heated/cooled plate wall temperature on the performance of latent heat storage system was investigated.

Most of the investigations on extended surfaces are generally focused on the finned surfaces in cylindrical geometries and investigations of rectangular fins in rectangular geometry are very few in number especially during the process of thermal energy release. The present work proposes to include horizontal fins in PCM to increase the heat exchange surface in order to enhance the heat transfer during the solidification process in a rectangular enclosure. The thermal behavior and thermal performance of the proposed system are studied numerically. Numerical investigations were carried out to study and examine the impact of the dimensionless fin length on the hydrodynamic and thermal fields of the flow, the heat transfer, the solidified mass fraction and the time of complete solidification.

## **2 Mathematical model**

The computational domain consists of a rectangular enclosure  $H \times L$ , shown in Fig. 1, including both the paraffin PCM (n-Octadecane) and horizontal fins of length,  $L_f$ , and thickness,  $e_f$ .

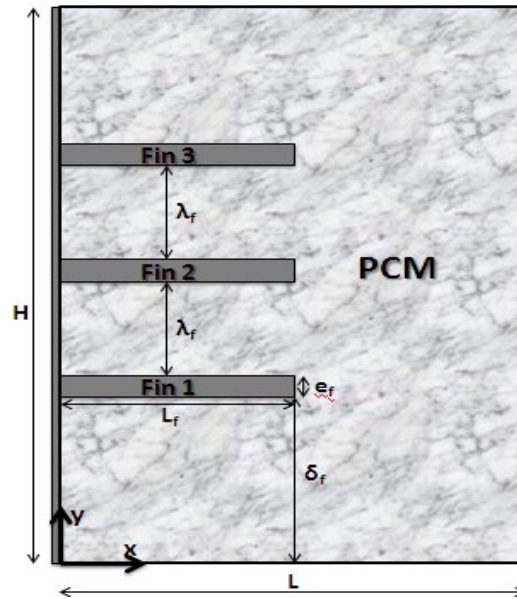


**Figure 1:** Schematic of the latent heat storage system

Initially, the PCM is superheated liquid. Its thermophysical properties are indicated in Tab. 1. The solidification is initiated by cooling the left finned wall. The other walls of the enclosure are adiabatic.

**Table 1:** Thermophysical properties of the PCM (n-Octadecane)

$T_m$ (K)	$k$ (W.m <sup>-1</sup> .K <sup>-1</sup> )	$\rho$ (kg.m <sup>-3</sup> )	$c$ (J.kg <sup>-1</sup> .K <sup>-1</sup> )	$\Delta H$ (kJ.kg <sup>-1</sup> )	$\mu$ (kg.m <sup>-1</sup> .s <sup>-1</sup> )	$\beta$ (K <sup>-1</sup> )
301.15	0.378	814	1900	243	$3.6 \times 10^{-3}$	$9.1 \times 10^{-4}$

### 2.1 Governing equations

The numerical analysis presented in this paper is based on a two-dimensional physical model. The modes of heat transfer considered here are heat conduction and natural convection. In this work the Boussinesq approximation is adopted and the viscous dissipation is neglected. The flow is assumed laminar and the liquid phase is Newtonian and incompressible. For the PCM, isotropic and homogeneous pure material properties are assumed. The thermophysical properties are independent of temperature and constant in the temperature range considered in the proposed study (255.16 K-323.16 K). The PCM properties are equal in the solid and liquid phase. The temperature and density references are calculated at melting point ( $T_{ref}=T_m$  and  $\rho_{ref}=\rho(T=T_m)$ ). The contact between the PCM and the solid boundaries is perfect and permanent.

Based on the above assumptions, a mathematical model incorporating conservation equations of mass ( $\Phi=1$ ), momentum ( $\Phi=U$  or  $V$ ) and energy ( $\Phi=\theta$ ), used for modeling the PCM solidification in a finned rectangular enclosure, are given by the general form of

dimensionless conservation equation as follow:

$$\frac{\partial(\Phi)}{\partial\tau} + \frac{\partial(U\Phi)}{\partial X} + \frac{\partial(V\Phi)}{\partial Y} = \Gamma \frac{\partial^2\Phi}{\partial X^2} + \Gamma \frac{\partial^2\Phi}{\partial Y^2} + S_\Phi \tag{1}$$

The quantities  $\Gamma$ ,  $\Phi$  and  $S_\Phi$  are given in Tab. 2.

**Table 2:** Quantities appearing in general Eq. (1)

$\Phi$	$\Gamma$	$S_\Phi$
1	0	0
U	Pr	$-\frac{\partial P}{\partial X} + S_U$
V	Pr	$-\frac{\partial P}{\partial Y} + S_V$
$\theta$	$\bar{\alpha}$	$S_\theta$

The equation of momentum ( $\Phi=U$  or  $V$ ) is similar to that of a porous medium with a porosity of zero in the solid areas and a porosity equal to one in the liquid zone. The terms  $S_U$  and  $S_V$  (Eqs. (2) and (3) below) appearing in this Eq. (1) are the source terms used to cancel the velocity in solid areas (solid PCM, walls and fins). The value of the constant “ $\bar{C}$ ” depends on the porous medium morphology. The quantity “ $b$ ” is introduced to avoid a division by zero in the case of zero liquid fraction.

The source term,  $S_\theta$  (Eq. (4)) is the driving force reflecting the phase change process, and the liquid fraction,  $f_l$ , reflects its evolution.

$$S_U = -\bar{C} \frac{(1-f_l)^2}{(f_l^3 + b)} U \tag{2}$$

$$S_V = -\bar{C} \frac{(1-f_l)^2}{(f_l^3 + b)} V + Ra Pr \theta \tag{3}$$

$$S_\theta = -\frac{1}{Ste} \frac{\partial f_l}{\partial \tau} \tag{4}$$

with:

$$Ra = \frac{g\beta l_0^3 (T_i - T_m)}{v_{m,l} \alpha_{m,l}}, Ste = \frac{c_{m,l} (T_i - T_m)}{\Delta H_m}, Pr = \frac{v_{m,l}}{\alpha_{m,l}}, \bar{\alpha} = 1 + (1 - f_l) \bar{\alpha}_s \quad (\bar{\alpha}_s = \frac{\alpha_{m,s}}{\alpha_{m,l}})$$

The above Eq. (1), was obtained in non-dimensional form by using the following dimensionless quantities:

$$X = \frac{x}{l_0}, Y = \frac{y}{l_0}, \tau = \frac{\alpha_{m,l} t}{l_0^2}, U = \frac{u}{\alpha_{m,l} / l_0}, V = \frac{v}{\alpha_{m,l} / l_0}, P = \frac{p}{\rho \left( \frac{\alpha_{m,l}}{l_0} \right)^2}, \theta = \frac{T - T_m}{T_i - T_m} \tag{5}$$

The quantity  $l_0 = \sqrt{H L - 3 L_f e_f}$  appearing in Eq. (5) is a reference length. It is chosen in such a way that its square is proportional to the mass of PCM, per unit of length, contained in the storage unit.

### **2.2 Boundary conditions**

The conservation equations are subject to the following initial and boundary conditions:

-Initial conditions:  $U = V = 0$ ,  $f_i = 1$  and  $\theta = \theta_i$ .

-Left wall-PCM interface:  $\theta_w = \theta = \theta_c$ .

-Fin-PCM interface:  $\theta_f = \theta = \theta_c$ .

-On the three adiabatic walls of the cavity:  $\frac{\partial \theta}{\partial \eta} = 0$

where  $\eta$  is the perpendicular direction to the wall of the enclosure.

-Non-slip and impermeability on all solid walls:  $U = V = 0$ .

As it can be seen, the governing parameters of the system are:

$$Ra, Ste, Pr, \overline{\alpha_s}, \theta_c, \overline{L_f} = \frac{L_f}{l_0}, \overline{\lambda_f} = \frac{\lambda_f}{l_0}, \overline{\delta_f} = \frac{\delta_f}{l_0}, A = \frac{H}{L}$$

### **2.3 Numerical methodology**

The enthalpy formulation [Voller, Cross and Markatos (1987)] is used to solve the problem of heat transfer with phase change. The equations of the mathematical model are discretized using the volume control method developed by Patankar [Patankar (1980)]. The algorithm SIMPLE (Semi Implicit Method for Pressure Linked Equation) [Patankar (1980)], is used to treat the pressure/velocity coupling. The resulting algebraic equations are solved using the algorithm of Thomas (TDMA) [Patankar (1980)].

A  $60 \times 80$  control volumes and time step of  $\Delta\tau = 3.4 \times 10^{-4}$  were obtained as optimal values for the present study. Numerical solution was declared converged when the relative change in the independent variables was lower or equal to  $10^{-9}$  and when mass and thermal balances were respectively lower or equal to  $10^{-8}$  and  $10^{-3}$ .

## **3 Results and discussion**

### **3.1 Example of simulation**

The numerical model was validated with numerical and experimental data published in Khatra et al. [Khatra and El Qarnia (2014); Khatra, El Qarnia, El Ganaoui et al. (2015)]. Numerical investigations were also carried out. The governing parameters are fixed to their reference values as given in Tab. 3.

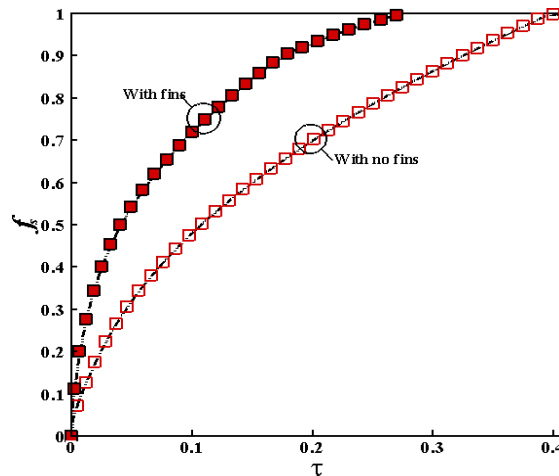
**Table 3:** The values of the governing control parameters

Ra	Ste	Pr	$\bar{\alpha}_s$	A	$\bar{\lambda}_f$	$\bar{L}_f$	$\bar{\delta}_f$	$\theta_C$
$3.92 \times 10^7$	0.172	18.09	1	4	0.33	0.25	0.66	-2.09

The values of  $l_o$  and  $l_{of}$  ( $l_{of} = \sqrt{\bar{L}_f e_f}$ ) are respectively equal to 0.06 m and 0.0067 m.

To highlight the effect of introducing horizontal rectangular fins into PCM on the evolution of the solidification process, numerical investigations were conducted to examine the thermal and hydrodynamic behavior of the finned and unfinned enclosures.

Fig. 2 displays the solidified mass fraction variations with time for finned and unfinned enclosures. As it can be seen from this figure, incorporation of fins in enclosure ensures a reduction in the time of complete solidification by 31%. The dimensionless times of complete solidification corresponding to unfinned and finned enclosures are 0.4 and 0.275, respectively.

**Figure 2:** Solidified mass fraction variations with time for finned and unfinned enclosures

To compare the heat fluxes extracted by the left finned and unfinned walls, the dimensionless heat flux variation with dimensionless time in the both cases is illustrated by Fig. 3(a). As depicted in this figure, the dimensionless heat flux,  $q$ , decreases with time and cancels in the end of the solidification process. Such a decrease is due to the increasing of the thermal resistance,  $R_{th}$ , of the solid PCM layer formed as the solid-liquid interface moves away from the left wall, as shown in Fig. 3(b). However, as compared to the case of unfinned enclosure, the case of finned enclosure presents lower thermal resistance and, then, higher dimensionless heat flux. This reveals that the heat transfer is better enhanced by the finned surface than by the plain one. This is due to the fact that introducing fins leads to an increase of heat exchange surface.

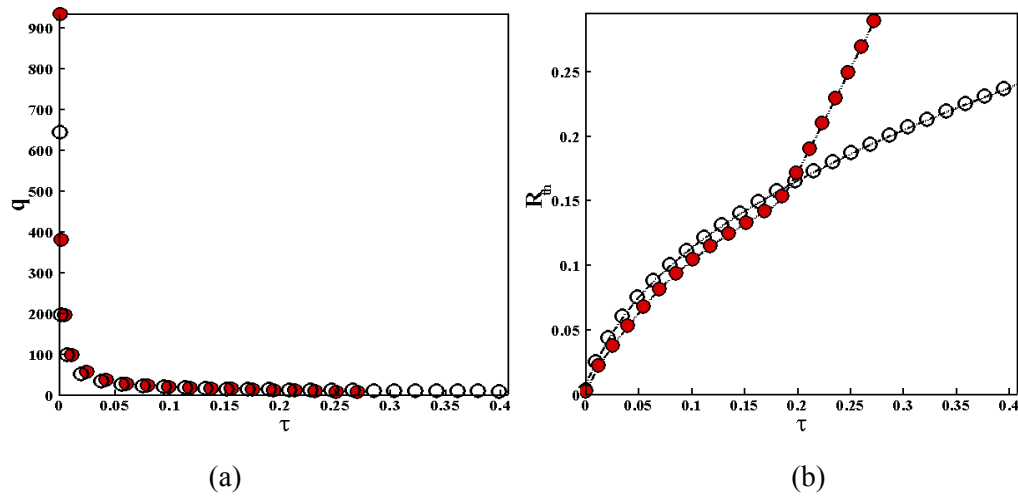


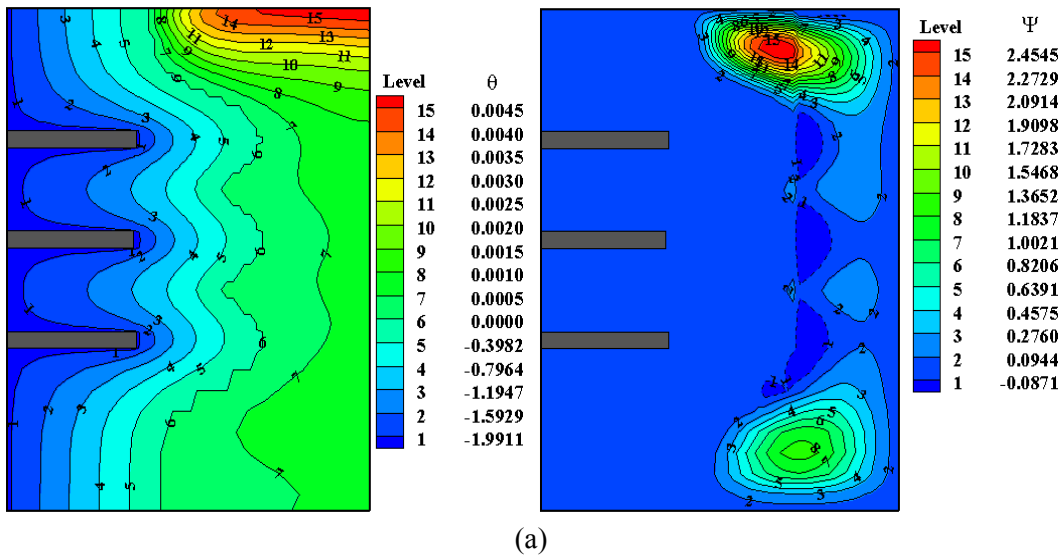
**Figure 3:** Dimensionless heat flux removed from PCM (a) and dimensionless thermal resistance of solid PCM (b) variations with time for unfinned (unfilled symbols) and finned (filled symbols) enclosure

### 3.2 The effect of the dimensionless fin length

The effect of the dimensionless fin length was studied by keeping other governing parameters fixed at their reference values as indicated in Tab. 3.

A comparative study of the solidification process was performed using fixed volumes of the PCM and fins for all numerical simulations ( $HL-3L_f e_f = l_0^2$  and  $L_f e_f = l_0 r^2$ ).

To highlight the effect of the dimensionless fin length on the hydrodynamic and thermal fields during the solidification process, Figs. 4 and 5 are included.



(a)

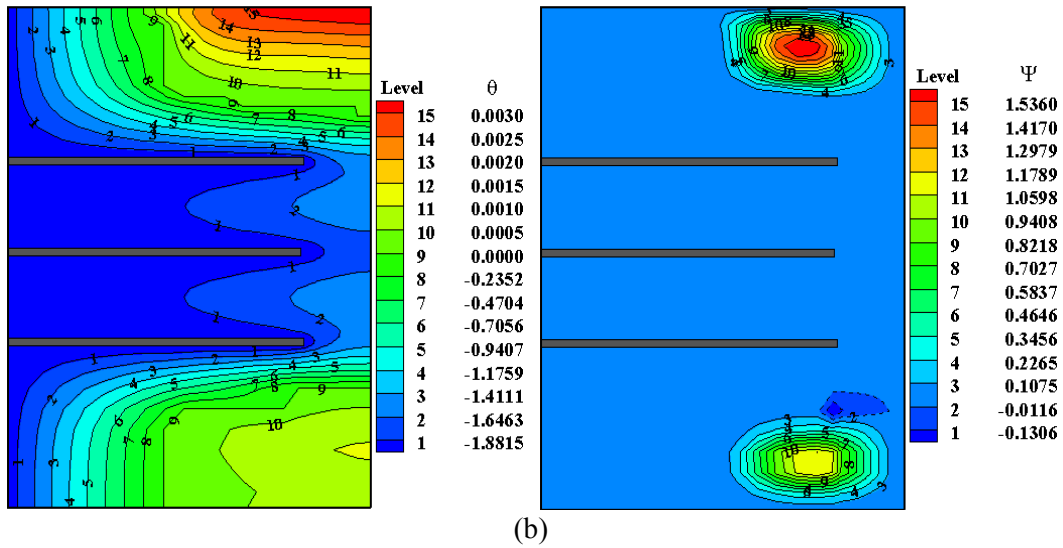


**Figure 4:** The effect of the dimensionless fin length (a:  $\bar{L}_f=0.18$ , b:  $\bar{L}_f=0.42$ ) on the hydrodynamic and thermal fields at the dimensionless time  $\tau=0.076$

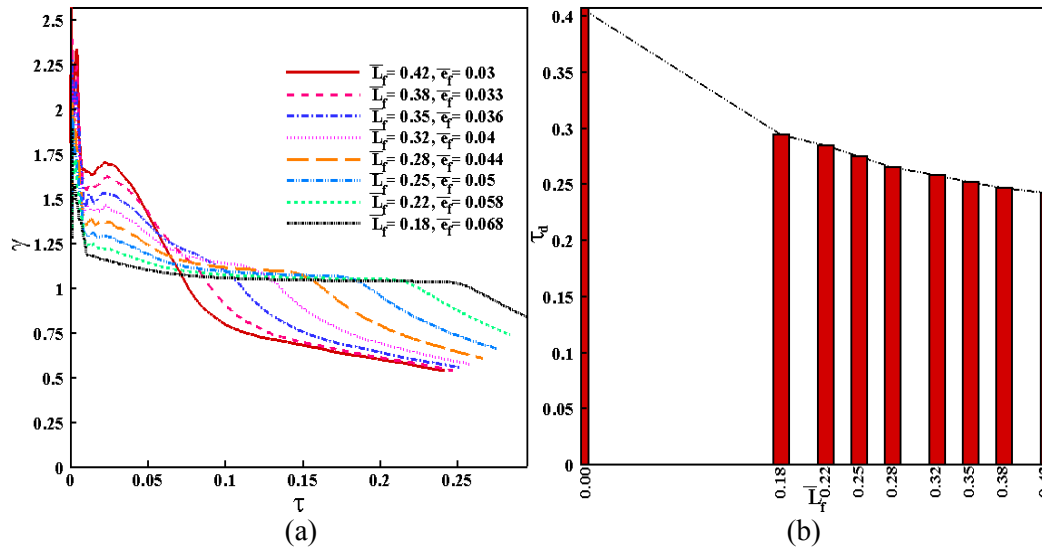


**Figure 5:** Variation of  $\gamma$  with time for different dimensionless fin lengths,  $\bar{L}_f$  (a) and the solidification time versus dimensionless fin length,  $\bar{L}_f$  (b)

Fig. 4 displays the streamlines ( $\Psi$ ) and the isotherms ( $\theta$ ) for two values of the dimensionless fin lengths  $\bar{L}_f=0.18$  (a) and  $\bar{L}_f=0.42$  (b) at the dimensionless time,  $\tau=0.076$ . This figure clearly showed that the isotherms in the solid phase are almost vertical at the top and the bottom parts of the enclosure while they are curved near fins.

This is due to the pure heat conduction in the solid phase. As it can be seen, for  $\overline{L}_f=0.18$ , two anti-clockwise rotating cells, separated by clockwise rotating cells, are developed at the upper and lower parts of the enclosure. The size and number of the two anti-clockwise rotating cells are reduced for higher dimensionless fin length ( $\overline{L}_f=0.42$ ). Besides, the liquid flow between the upper and lower rotating cells near the right side wall, which is appeared for  $\overline{L}_f=0.18$ , disappears when the dimensionless fin length increases. This effect weakens the convection movement caused by the natural convection. In addition, longer fins offer more heat exchange surface and hence more heat extraction from the liquid PCM. These two effects promote solidification process.

To show the effect of fins on the dimensionless heat flux extracted by the left vertical wall of the enclosure, the ratio  $\gamma$  (ratio of the dimensionless heat flux for the case of finned enclosure to the dimensionless heat flux for the case of unfinned enclosure) has been calculated. Fig. 5(a) shows the variations of the ratio,  $\gamma$ , with the dimensionless time, for different values of the dimensionless fin length. It is clear that at the beginning of the solidification process, the ratio,  $\gamma$ , is greater than 1 for all fin length values; its value, e.g., for  $\overline{L}_f=0.25$ , is increasing up to 1.96 and decreases rapidly before reaching a value of 1.07. This behavior can be explained by the fact that the heat transfer is intensified by fins which increase heat exchange surface. As it can be seen, higher values of the ratio  $\gamma$  are obtained in the beginning of the solidification process for higher dimensionless fin length. It is obvious, because when increasing the dimensionless length of fin, the heat exchange surface increases and hence the dimensionless heat flux extracted from the finned left wall increases compared to the case of unfinned left wall. However, at the end of the solidification process for the case of finned enclosure, the dimensionless thermal resistance exceeds that associated to unfinned case (as already mentioned in Section 3.1 Fig. 3(b)). This is the reason behind the abrupt drops of the ratio  $\gamma$ . The more the fin is longer, the more the drop of the ratio  $\gamma$  is fast. Then, with longer fins the solidification process is accelerated and complete solidification time is reduced. This result can be observed in Fig. 5(b), which presents the variation of the dimensionless solidification time,  $\tau_d$ , with the dimensionless fin length ( $\overline{L}_f=0.0$  correspond to the case of without fins), the solidification time is reduced by 40.5%, in the range of the dimensionless fin length explored in this study.

#### **4 Conclusion**

A mathematical model has been developed to study the solidification process of the PCM inside a rectangular enclosure provided with internal rectangular fins. The governing parameters were identified and several numerical investigations were conducted to study the effect of the dimensionless fin length on the hydrodynamic and thermal fields and also the thermal performance. The following conclusions can be drawn:

- A comparative study between two enclosures with and without fins showed that the time of complete solidification can be reduced and the removed heat flux can be improved by introducing fins;

- Longer fins weaken the natural convection in the liquid layer and offer more heat exchange surface. This effect increases the ratio,  $\gamma$ , which means that the dimensionless heat flux extracted by the left finned wall is improved and then solidification process is accelerated;
- In the range of the dimensionless fin lengths explored in this study, the solidification time is reduced by 40.5%.

Further researches are needed to investigate on the optimum geometrical parameters of the fins and enclosure for enhancing the solidification rate and minimizing the complete solidification time.

### References

**Arid, A.; Kousksou, T.; Jegadheeswaran, S.; Jamil, A.; Zeraouli, Y.** (2012): Numerical simulation of ice melting near the density inversion point under periodic thermal boundary conditions. *Fluid Dynamics and Material Processing*, vol. 8, no. 3, pp. 257-275.

**Bauer, T.** (2011): Approximate analytical solutions for the solidification of PCMs in fin geometries using effective thermophysical properties. *International Journal of Heat and Mass Transfer*, vol. 54, pp. 4923-4930.

**Ismail, K. A. R.; Alves, C. L. F.; Modesto, M. S.** (2001): Numerical and experimental study on the solidification of PCM around a vertical axially finned isothermal cylinder. *Applied Thermal Engineering*, vol. 21, no. 1, pp. 53-77.

**Jegadheeswaran, S.; Pohekar, S. D.** (2009): Performance enhancement in latent heat thermal storage system: a review. *Renewable and Sustainable Energy Reviews*, vol. 13, no. 9, pp. 2225-2244.

**Khatra, L.; El Qarnia, H.** (2014): Validation of numerical study of solidification of phase change material in rectangular enclosure with fins. *Proceedings of ASME Verification and Validation Symposium (V&V2014-7099)*, Tropicana Las Vegas, Las Vegas, Nevada.

**Khatra, L.; El Qarnia, H.; El Ganaoui, M.; Lakhali, El-K.** (2015): Numerical investigation of heat transfer during solidification in a rectangular enclosure with internally horizontal partial fins. *Computational Thermal Sciences*, vol. 7, no. 4, pp. 293-312.

**Patankar, S. V.** (1980): *Numerical Heat Transfer and Fluid Flow*. Hemisphere, Washington, D.C.

**Rady, M.; Arquis, E.** (2010): A comparative study of phase changing characteristics of granular phase change materials using DSC and T-History Methods. *Fluid Dynamics and Material Processing*, vol.6, no. 2, pp. 137-152.

**Semma, E. A.; El Ganaoui, M.; Timchenko, V.; Leonardi, E.** (2006): Some thermal modulation effects on directional solidification. *Fluid Dynamics and Material Processing*, vol. 2, no. 3, pp. 191-202.

**Stritih, U.** (2004): An experimental study of enhanced heat transfer in rectangular PCM storage. *International Journal of Heat and Mass Transfer*, vol. 47, no. 12, pp. 2841-2847.

**Velraj, R.; Seeniraj, R. V.; Hafner, B.; Faber, C.; Schwarzer, K.** (1997): Experimental analysis and numerical modelling of inward solidification on a finned vertical tube for a latent heat storage unit. *Solar Energy*, vol. 60, no. 5, pp. 281-290.

**Voller, V. R.; Cross, M.; Markatos, N. C.** (1987): An enthalpy method for convection/diffusion phase change. *International Journal for Numerical Methods in Engineering*, vol. 24, no. 1, pp. 271-284.

**Ye, W. B.; Zhu, D. S.; Wang, N.** (2011): Numerical simulation on phase-change thermal storage/release in a plate-fin unit. *Applied Thermal Engineering*, vol. 31, pp. 3871-3884.